BIOCHEMISTRY
including biophysical chemistry & molecular biology

Article

pubs.acs.org/biochemistry

A Buried Ionizable Residue Destabilizes the Native State and the Transition State in the Folding of Monellin

Nilesh Aghera, Ishita Dasgupta, and Jayant B. Udgaonkar*

National Centre for Biological Sciences, Tata Institute of Fundamental Research, Bangalore 560065, India

ABSTRACT: A buried ionizable residue can have a drastic effect on the stability of a native protein, but there has been only limited investigation of how burial of an ionizable residue affects the kinetics of protein folding. In this study, the effect of burial of ionizable residues on the thermodynamics and kinetics of folding and unfolding of monellin has been investigated. The stability of wild-type (wt) monellin is known to decrease with an increase in pH from 4 to 10. The Glu24 → Ala mutation makes the stability of the resultant E24A mutant protein independent of pH in the range from 4 to 8. An additional mutation, Cys42 → Ala, results in the stability becoming independent of pH in the range from 4 to 10. Like the wt protein, E24A folds via very fast, fast, and slow folding pathways. Compared to that of the wt protein, the rate of slow folding pathway of E24A is ∼7-fold faster, the rate of fast folding pathway is ∼1.5-fold faster, while the rate of very fast folding pathway is similar. E24A unfolds ∼7-fold slower than the wt. The extent of stabilization of the transition state (TS) observed for the slow pathway of refolding and for unfolding is the same, indicating that unfolding occurs via the TS populated on the slow pathway of refolding. The stabilization of the TS of folding (1.1 kcal mol^{-1}) is less than that of the native state (2.3 kcal mol^{-1}) of E24A, indicating that structure has only partially formed in the vicinity of Glu24 in the TS of folding.

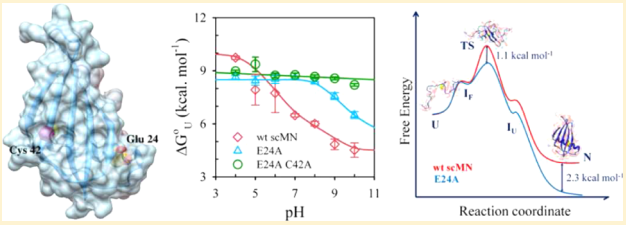

Hydrophobic interactions, conformational entropy, and hydrogen bonding are believed to contribute most to protein stability,[1−5] but electrostatic interactions also play a crucial role in determining protein stability.[6−9] The contribution of electrostatic interactions to stability depends strongly on their environment inside and outside the protein.[10−14] An important modulator of electrostatic interactions is pH, which is known to affect protein stability in diverse ways. A protein may unfold at acidic and basic pH because some groups in the protein may preferentially bind protons in the unfolded state versus the native state at acidic pH, and other groups may preferentially bind protons in the native state versus the unfolded state at basic pH.[15,16] If a protein has an ionizable residue buried in its hydrophobic core, it may display a pH-dependent change in its stability.[17−21] An amino acid residue experiences a large change in the polarizability of its environment when it moves from the solvent to the interior of the protein upon folding. For an ionizable residue, this can cause a shift in its pK_a: an acidic residue would show an increase in its pK_a value,[19,22−24] while a basic residue would show a decrease in its pK_a value.[25−27] Because of the shift in its pK_a, the ionizable residue titrates differently in the native and unfolded states, giving rise to a pH-dependent change in protein stability. The shift in the pK_a of a buried residue can be probed using nuclear magnetic resonance (NMR) spectroscopy,[23,28] or by mutagenesis studies.[18−20]

When the folding process involves burial of an ionizable residue, the stability of the protein may be affected in addition to the kinetics of folding of the protein. When burial does result in the pK_a of an ionizable residue being different in the native and unfolded states, it becomes important to understand the point during the folding process at which the pK_a value of an ionizable group shifts from its value in the unfolded protein to its value in the folded protein. Understanding the process of burial of an ionizable residue in the core of a protein may help in delineating the folding mechanism of the protein at the residue level. Removal of a buried ionizable residue from the hydrophobic core of a protein by mutation is known to stabilize the native state.[21,22] If a mutation stabilizes only the native state and does not stabilize the transition state (TS), the free energy barrier to unfolding will be larger and unfolding slower. If the mutation stabilizes both the native state and the TS and does not perturb the energetics of the unfolded state, then the folding rate will increase. Comparative kinetic studies of the two forms of the protein, with and without a buried ionizable group, can provide insight into the temporal events of structure formation around the specific residue during the folding process.

To understand how a buried ionizable residue affects the thermodynamics and kinetics of protein folding and/or unfolding, we have used the small plant protein monellin as a model system. Both the monomeric (scMN)[29−32] and dimeric (dcMN)[32−35]forms of monellin have been used extensively to understand the thermodynamics and kinetics of its folding and unfolding. In a previous study, it was shown that the stability of scMN as well as that of dcMN changes in a pH-dependent manner.[32] It appeared that the pH-dependent change in the stability arose from the titration of a buried Asp or Glu side chain, whose pK_a value had shifted from a value of ∼4 in the unfolded state to a value of ∼9.5 in the native state. An inspection of the

Received: June 15, 2012
Revised: August 29, 2012
Published: October 22, 2012

dx.doi.org/10.1021/bi3008017 | *Biochemistry* 2012, 51, 9058−9066

crystal structure of monellin using computational tools had suggested that the buried ionizable residue could be either Glu24 or Glu78 (Figure 1).

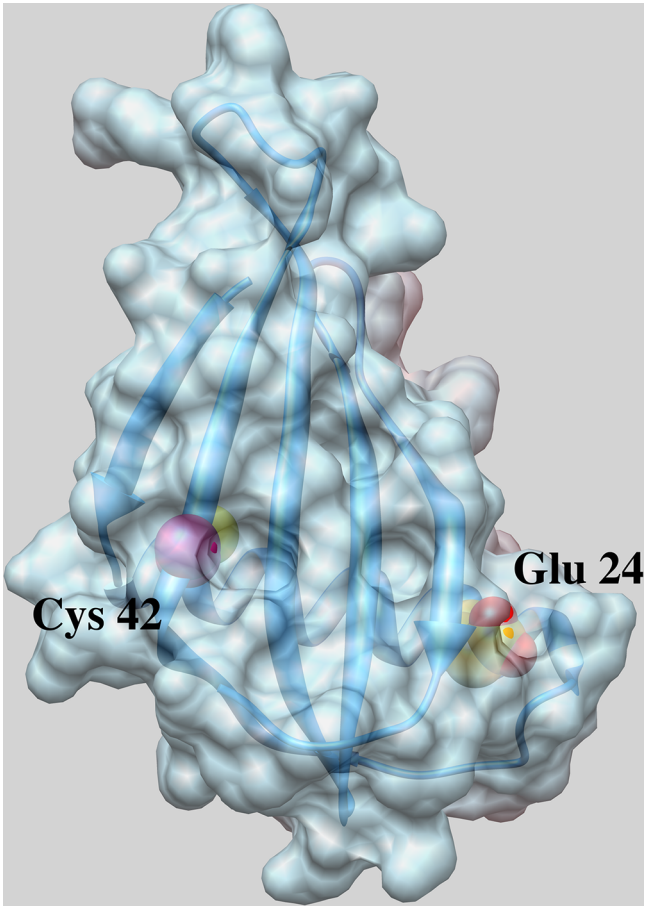

Figure 1. Structure of single-chain monellin showing the positions of the mutated residues. Glu24 (gold) and Cys42 (purple) were both mutated to alanine. The protein has 53 ionizable residues and 78 ionizable groups. Only three ionizable residues, Glu24, Cys42, and Thr13, exhibit <10% solvent accessibility for the polar moieties of their side chains. This image was produced using the UCSF Chimera package from the Resource for Biocomputing, Visualization, and Informatics at the University of California, San Francisco (supported by National Institutes of Health Grant P41 RR001081) from Protein Data Bank entry 1IV7.

In this study, we show, by individually replacing both Glu24 and Glu78 with Ala, that Glu24 is the key residue determining the pH dependence of stability in the pH range of 4−8. The E24A mutant protein shows, however, a decrease in stability with a change in pH from 8 to 10. Again, site-directed mutagenesis shows that the decrease in the stability of the protein from pH 8 to 10 arises because of the presence of the buried Cys42 residue. The E24A/C42A double-mutant protein does not show a change in stability with a change in pH from 4 to 10. Kinetic studies performed with the E24A mutant protein show that its folding rate is increased and its unfolding rate is decreased. The observed increase in the folding rate is shown to arise due to the partial stabilization of the TS relative to the native state.

MATERIALS AND METHODS

Reagents. All the reagents used in the experiments were from Sigma and were of the highest purity grade. GdnHCl was purchased from USB and was of the highest purity grade.

Preparation of scMN. The method for the purification of monellin has been described previously.[29,36] Three mutant variants of monellin were studied: E24A with the Glu24 → Ala mutation, E78A with the Glu78 → Ala mutation, and E24A/C42A with the Glu24 → Ala and Cys42 → Ala mutations. All the mutant proteins were purified using the same protocol without any modification. The purity of the proteins was confirmed by sodium dodecyl sulfate−polyacrylamide gel electrophoresis and mass spectrometry.

CD Measurements. CD spectra were collected using a Jasco J-815 spectropolarimeter. Far-UV CD spectra were acquired using a protein concentration of 10 μM in a 0.1 cm cuvette, using a scan speed of 50 nm/min and a digital integration time of 2 s. CD spectra were acquired at a bandwidth of 1 nm.

Equilibrium Unfolding Studies. GdnHCl-induced equilibrium unfolding transitions were monitored by measurement of the change in the intrinsic tryptophan fluorescence, using the MOS 450 optical system from Biologic. The protein sample was excited at 280 nm, and emission was collected at 340 nm using a 10 nm band-pass filter (Asahi Spectra). Equilibrium unfolding studies were performed in the pH range of 4−10. All the equilibrium unfolding studies were performed in a narrow protein concentration range of 5−10 μM. The buffer strength at all pH values was kept constant; 50 mM sodium acetate buffer was used at pH 4 and 5, 50 mM sodium phosphate buffer at pH 6 and 7, 50 mM Tris buffer at pH 8 and 9, and 50 mM sodium borate buffer at pH 10. In addition, each buffer contained 0.25 mM EDTA and 1 mM DTT. At each pH, the protein was incubated in different concentrations of GdnHCl, for 18 h, until equilibrium was established, before measurement of the fluorescence signal.

Unfolding Kinetics. The unfolding kinetics was monitored by measurement of the change in tryptophan fluorescence at 340 nm upon excitation at 280 nm, using the MOS 450 optical system coupled to a stopped-flow module (SFM400) from Biologic. The dead time of mixing on the SFM400 was 12 ms. Unfolding kinetic studies at low denaturant concentrations were performed by manual mixing with a dead time of 10 s. Unfolding studies were conducted at a protein concentration of 10 μM and in the GdnHCl concentration range of 3.5−6 M.

Refolding Kinetics. Refolding kinetic studies were performed using the SFM4 stopped-flow module from Biologic. Refolding was monitored by measurement of the change in the intrinsic tryptophan fluorescence. The protein was excited at 280 nm, and emission was monitored at 340 nm using a band-pass filter (Asahi Spectra). The protein was kept unfolded for 6 h before the refolding experiments were performed. The refolding of the protein was initiated by diluting unfolded protein in the presence 4 M GdnHCl to different final concentrations of GdnHCl by appropriate dilution.

Analysis of Equilibrium Unfolding Curves. A two-state N ↔ U model was used for the analysis of the equilibrium unfolding of scMN, as described previously.[29,37]

When two titratable groups in a protein have different pK_a values in the N (pK_{a1}^{N} and pK_{a2}^{N}) and U forms (pK_{a1}^{U} and pK_{a2}^{U}), then the linkage between folding and proton binding yields the following expression for the dependence of the apparent free energy of unfolding, $\Delta G^{o,app}_{U}$, on pH:

dx.doi.org/10.1021/bi3008017 | *Biochemistry* 2012, 51, 9058−9066

$$\Delta G_U^{o,app} = \Delta G_U^o - 2.3RT \log\left[\left(\frac{1 + 10^{(pK_{a1}^U - pH)}}{1 + 10^{(pK_{a1}^N - pH)}}\right) \times \left(\frac{1 + 10^{(pK_{a2}^U - pH)}}{1 + 10^{(pK_{a2}^N - pH)}}\right)\right] \quad (1)$$

where ΔG°_{U-N} is the free energy of unfolding of the protein with both titratable groups deprotonated in N as well as in U.

Analysis of Unfolding Kinetics. The unfolding mechanism of scMN can be represented by the simple mechanism N ↔ I_U ↔ U, where the intermediate ensemble I_U is composed of at least two subpopulations of molecules.[30,31] When I_U is formed rapidly from N so that a pre-equilibrium, defined by the equilibrium constant K_{NI}, is established between N and I_U before further unfolding occurs, the observed unfolding rate constant λ_U is given by

$$\lambda_U = \frac{K_{NI}}{K_{NI} + 1} k_{IU} \quad (2)$$

k_{IU} is the rate constant of unfolding of I_U.

When $K_{NI} < 1$

$$\lambda_U = K_{NI} k_{IU} \quad (3)$$

The dependence of λ_U on denaturant concentration, [D], is given by

$$\ln \lambda_U = \ln \lambda_U^{H_2O} + m_{\ddagger-N}[D] \quad (4)$$

where $m_{\ddagger-N}$ is proportional to the difference in surface area between N and the TS of unfolding.

Analysis of Folding Kinetics. In previous studies, it was established that the folding of monellin commences with a submillisecond kinetic phase[29,38] leading to a collapsed intermediate ensemble.[29,39] The subpopulations in this collapsed intermediate ensemble fold via independent pathways.[29,39] Each of these pathways can be represented by the scheme U ↔ I_F ↔ N. In this scheme, the very rapid formation of I_F leads to a pre-equilibrium defined by the equilibrium constant K_{UI} being established between U and I_F, before further folding of I_F occurs. If the rate constant for the disappearance of I_F is k_{IN}, then the observed rate constant for each of the three kinetic phases is

$$\lambda_f = \frac{K_{UI}}{K_{UI} + 1} k_{IN} \quad (5)$$

When $K_{UI} < 1$

$$\lambda_f = K_{UI} k_{IN} \quad (6)$$

The dependence of λ_f on denaturant concentration is given by

$$\ln \lambda_f = \ln \lambda_f^{H_2O} + m_{\ddagger-U}[D] \quad (7)$$

where $m_{\ddagger-U}$ is proportional to the difference in surface area between U and the TS of folding.

RESULTS

Equilibrium Unfolding of scMN, E24A, and E24A/C42A. GdnHCl-induced equilibrium unfolding curves for wt scMN, E24A and E24A/C42A were determined at different pH values in the pH range of 4−10. Figure 2a shows that the stabilities of wt scMN, E24A, and E24A/C42A are similar at pH 4: the midpoints (C_m) of the equilibrium unfolding curves are very close in value to each other. Figure 2b shows that the stability of wt scMN is much lower at pH 10 than at pH 4, in agreement with earlier work.[32] The stability of E24A is also reduced at pH 10, although to a smaller extent compared to the decrease in stability of wt scMN. On the other hand, the stability at pH 10 of the E24A/C42A double mutant remains the same as the stability at pH 4.

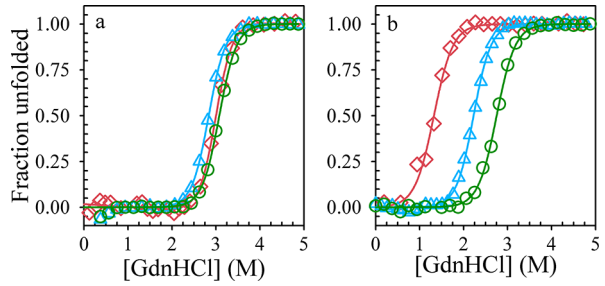

Figure 2. Equilibrium unfolding transitions of mutant and wild-type scMN. The GdnHCl-induced equilibrium unfolding transitions were monitored by measurement of the change in fluorescence at 340 nm for the wild type (red ◇), E24A (blue △), and E24A/C42A (green ○) at pH 4 (a) and pH 10 (b). The plots of f_U vs GdnHCl concentration were obtained from the raw data as described previously.[32] The solid lines through the data are nonlinear least-squares fits to the equation for a two-state unfolding model,[37] and the values obtained for ΔG_U and m_U are shown in Figure 3.

pH Dependence of the Stabilities of wt scMN and Mutants E24A and E24A/C42A. Figure 3 shows the pH dependencies of the thermodynamic parameters governing the unfolding of wt scMN, E24A, and E24A/C42A. At pH 4 and 5, the stability of wt scMN is marginally higher than the stabilities of the mutant variants. The stability of wt scMN decreases above pH 5 and reaches its minimal value at pH >9. In contrast, the stability of E24A decreases only above pH 8, while the stability of E24A/C42A appears not to change in the pH range of 4−10. For all three proteins, the values of m_U are the same and do not change with pH (Figure 3b). As expected, the pH dependencies of the C_m values mirror those of the ΔG°_U values (data not shown).

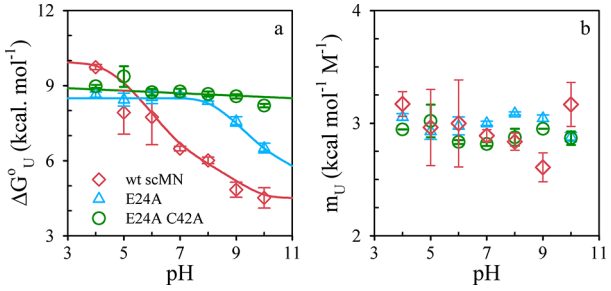

Figure 3. pH dependence of thermodynamic parameters governing the unfolding of wt scMN (red ◇), E24A (blue △), and E24A/C42A (green ○). Panels a and b show the values of the thermodynamic parameters ΔG°_U and m_U, respectively, obtained by analyzing the equilibrium unfolding transitions using a two-state N ↔ U model.[37] The solid lines through the parameters for wt scMN were drawn using eq 1. The solid lines through the parameters for mutants E24A and E24A/C42A were drawn by inspection only. Error bars, wherever shown, represent the spreads of the measurements taken in at least two independent experiments.

The data in Figure 3a clearly implicate Glu24 and Cys42 as the residues responsible for the dependence of the stability of wt scMN on pH. Each of these two buried residues (see Figure 1) can be expected to have a higher pK_a value in the native state than in the unfolded state. Equation 1 (see Materials and Methods)

dx.doi.org/10.1021/bi3008017 | Biochemistry 2012, 51, 9058−9066

describes the pH dependence of stability for a protein in which two ionizable groups each have different pK_a values in the native and unfolded states. Figure 3a shows that eq 1 can account for the observed pH dependence of the stability of wt scMN, when the pK_a values of Glu24 and Cys42 are taken to be 4.5 and 8.5, respectively, in the unfolded state and 7.5 and 9.5, respectively, in the native state. While the values assumed for the unfolded state are the values expected for the free amino acids in water, the values assumed for the native state are merely the minimal estimates: lower values for the native state do not describe the data well. The quality of data does not allow reliable pK_a values to be extracted using eq 1.

The pH dependence of the stability of E78A was found to be very similar to that of wt scMN (data not shown), indicating that the pK_a of Glu78 is not different in the N and U states. Although Glu78 is fully buried, three Arg residues, Arg54, Arg83, and Arg85, are nearby (within 6 Å) in the structure. Hence, the increase in the pK_a of Glu78 caused by burial in the native protein appears to be compensated for by its proximity to the arginine residues.

E24A/C42A Retains Native Structure at pH 12. It is known that wt scMN unfolds completely at pH 12.[39] Figure 4 shows that while the far-UV CD spectra of wt scMN and E24A/C42A are identical at pH 7, the far-UV CD spectra of the two protein variants are different at pH 12. While the far-UV CD spectrum of wt scMN at pH 12 indicates that most, if not all, of its secondary structure is lost, the far-UV CD spectrum of E24A/C42A at pH 12 is similar to that of the protein at pH 7, indicating that E24A/C42A remains fully folded at pH 12.

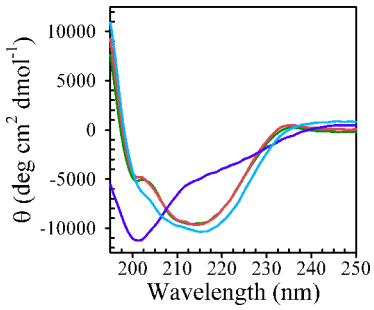

Figure 4. Structural characterization of scMN and E24A/C42A at pH 7 and 12. Far-UV CD spectra of wt scMN acquired at pH 7 (green) and pH 12 (blue) and of E24A/C42A acquired at pH 7 (red) and pH 12 (light blue) are shown.

E24A Unfolds Slower Than wt scMN at pH 7. Figure 5a shows representative kinetic unfolding traces of E24A monitored by measurement of intrinsic tryptophan fluorescence. As in the case of wt scMN,[29] the kinetic traces at all GdnHCl concentrations are described well by a single-exponential equation, and they all originate at a fluorescence value 10−15% higher than that of the native protein. This becomes obvious when the kinetic amplitudes of unfolding are compared to the equilibrium amplitudes (Figure 5b). Like in the case of wt scMN,[29] the kinetic traces of unfolding of E24A start at a value of fluorescence higher than that of the folded protein; nevertheless, the starting points are below the values expected from linear extrapolation of the folded protein baseline. Figure 5c and Table 1 show that E24A unfolds slower than wt scMN, and that the unfolding rate constant of E24A has the same dependence on GdnHCl concentration as that of wt scMN. Table 2 shows that the Glu24 → Ala mutation stabilizes the native state of the protein by 2.3 kcal mol^{-1} at pH 7 but stabilizes the TS of unfolding by only 1.1 kcal mol^{-1}.

E24A Folds Faster Than wt scMN at pH 7. The change in fluorescence accompanying the refolding of wt scMN at pH 7 is known to occur in three observable phases:[29] very fast (108 s^{-1}), fast (8 s^{-1}), and slow (0.6 s^{-1}). The same kinetic phases are seen during the folding of E24A, but in addition, some of the fluorescence change also occurs during a 6 ms burst phase (Figure 6a). The relative amplitude of the burst phase change in fluorescence increases with a decrease in GdnHCl concentration (Figure 6b). For each of the three observable kinetic phases, the plot of log(λ) versus GdnHCl concentration is linear (Figure 6c). The values of the observed rate constants in the absence of denaturant, as well as the dependencies of the observed rate constants on GdnHCl concentration, are listed in Table 1. Table 1 also lists the corresponding values for wt scMN.[29] It is seen that the observed rate constant for the very fast phase is unaffected by the mutation, while the observed rate constants for the fast and slow phases are ∼1.5- and ∼7-fold faster, respectively, for E24A than for wt scMN. Figure 6d shows that the relative amplitudes of the three observable phases do not change appreciably with a change in GdnHCl concentration.

Table 2 shows that the TS for the slow phase of folding is stabilized by 1.2 kcal mol^{-1}. The TS for very fast phase is not stabilized, and that for the fast phase is only marginally stabilized (see the data in Table 1).

DISCUSSION

Because of the high energetic cost of transferring a charge from a polar to a nonpolar environment,[40−43] ionizable amino acid residues are usually not found in their charged states in the interiors of proteins[44,45] unless they are functionally important.[46−50] Quite predictably, a proteome wide analysis has revealed that most buried ionizable groups in proteins are electrostatically optimized for the formation of polar interactions.[51,52] When a buried ionizable residue in the core of a protein does not make any polar interactions, it can destabilize the protein in a pH-dependent manner.[17−20] In this study, the pH dependence of the stability of monellin is attributed to the ionization of the buried residues, Glu24 and Cys42.

Glu24 Has an Increased pK_a in the Native State. Glu24 is located at the C-terminal end of the sole α-helix of scMN (Figure 1). It has >95% of its total surface area buried in the core of the protein. The ionizable moiety of the side chain has 6% of its surface area accessible to water, with one oxygen atom being completely buried, while the other has 10% solvent accessibility. The polar moiety of the Glu24 side chain is ∼5.9 Å from the protein surface, as computed using DEPTH.[53] The microenvironment of Glu24 is predominantly hydrophobic. Its two adjacent residues, Glu23 and Asn25, have their side chains oriented away from the Glu24 side chain.

The stability of the E24A mutant is independent of pH in the pH range of 4−8, but the protein shows a gradual decrease in stability from pH 8 to 10 (Figure 3). The data also indicate that the ionization of Glu24 is not responsible for the decrease in stability seen for wt scMN at higher pH values (>8). Large shifts in pK_a values such as that observed for Glu24 have also been observed for other proteins.[20,54−56] It should be noted that only an approximate value can be obtained for the pK_a of Glu24 in the native state (see Results) from the pH dependence of stability, and NMR measurements would be necessary to obtain a more reliable value for the pK_a.

dx.doi.org/10.1021/bi3008017 | *Biochemistry* 2012, 51, 9058−9066

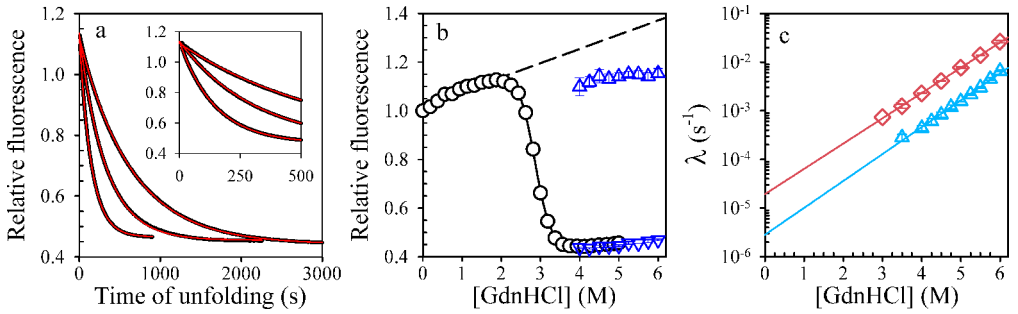

Figure 5. Unfolding kinetics of E24A at pH 7. Unfolding was monitored by measurement of the change in tryptophan fluorescence at 340 nm. (a) Representative unfolding kinetic traces (solid black lines) obtained when the native protein was unfolded at final GdnHCl concentrations of 5, 5.5, and 6 M (from right to left, respectively). The red lines through the curves represent nonlinear least-squares fits to a single-exponential equation. The inset shows the initial parts of the unfolding kinetic traces. (b) Comparison of kinetic and equilibrium amplitudes. The equilibrium unfolding curve (○) of E24A and the fit through the data using the equation for a N ↔ U two-state model (solid black line) [t = 0 points (blue △) and t = ∞ points (blue ▽)], obtained by fitting the unfolding kinetic traces of E24A. The dashed black line represents the extrapolated native protein signals at different GdnHCl concentrations. (c) Observed unfolding rate constants for wt scMN (red ◇) and E24A (light blue △). The solid black lines represent nonlinear least-squares fits to eq 4. The values obtained for λ_U in water and for $m_{\ddagger-N}$ are listed in Table 1. Error bars, wherever shown, represent the spreads in the measurements taken in at least two separate experiments.

Table 1. Kinetic Parameters Governing Folding and Unfolding at pH 7

		parameters	wt scMN	E24A
folding	very fast phase	λ_f^{vf} (s^{-1})	108	108
		$m_{\ddagger-U}^{vf}$ (kcal mol^{-1} M^{-1})	−3.1	−2.6
	fast phase	λ_f^{f} (s^{-1})	8.0	12.4
		$m_{\ddagger-U}^{f}$ (kcal mol^{-1} M^{-1})	−3.0	−2.5
	slow phase	λ_f^{S} (s^{-1})	0.6	4.4
		$m_{\ddagger-U}^{s}$ (kcal mol^{-1} M^{-1})	−2.4	−2.8
unfolding		λ_u (s^{-1})	2×10^{-5}	3×10^{-6}
		$m_{\ddagger-N}$ (kcal mol^{-1} M^{-1})	0.7	0.7

Table 2. Comparison of the Thermodynamic Parameters Governing Unfolding, Obtained from Equilibrium and Kinetic Studies at pH 7[a]

	parameters	wt scMN	E24A
equilibrium measurements	ΔG^{o}_{U} (kcal mol^{-1})	6.3	8.6
	m_U (kcal mol^{-1} M^{-1})	2.7	3.0
	$\Delta\Delta G^{o}_{U}$ (kcal mol^{-1})		2.3
kinetic measurements	$\Delta G^{o}_{U} = -RT \ln(\lambda_U/\lambda_f^{s})$ (kcal mol^{-1})	6.1	8.4
	$\Delta\Delta G^{o}_{U}$ (kcal mol^{-1})		2.3
	$m_U = m_{\ddagger-N} + (-m_{\ddagger-U}^{S})$ (kcal mol^{-1} M^{-1})	3.2	3.5
	$\Delta\Delta G_{\ddagger-N} = -RT \ln(\lambda_U^{wt}/\lambda_U^{mut})$ (kcal mol^{-1})		−1.2
	$\Delta\Delta G_{\ddagger-U} = -RT \ln(\lambda_f^{wt}/\lambda_f^{mut})$ (kcal mol^{-1})		1.1

[a]The values of ΔG^{o}_{U} were obtained either from the two-state analysis of the equilibrium unfolding transitions (equilibrium measurements) or from the values of the rates of unfolding and folding of the slow phase [kinetic measurements (Table 1)]. The value of $\Delta\Delta G^{o}_{U}$ represents the change in the free energy of unfolding upon mutation of Glu24 to Ala, calculated by subtracting the free energy of unfolding of the wild-type protein from that of the E24A mutant. The $\Delta\Delta G^{o}_{U}$ value is calculated for the slow pathway of refolding. All the values used to calculate the parameter for the kinetic measurements are listed in Table 1.

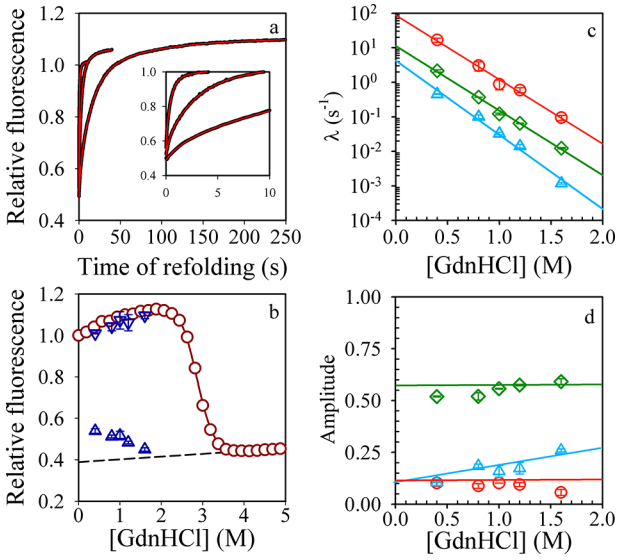

Figure 6. Refolding kinetics of E24A at pH 7. Refolding was monitored by measurement of the change in the intrinsic tryptophan fluorescence at 340 nm. (a) Representative refolding kinetic traces (—) obtained by diluting the unfolded protein in 4 M GdnHCl to final denaturant concentrations of 0.4, 0.8, and 1 M GdnHCl (from left to right, respectively). The lines through the curves represent nonlinear least-squares fits to a three-exponential equation. The inset shows the initial parts of the refolding kinetic traces. (b) Comparison of the kinetic and equilibrium amplitudes [(red ○) equilibrium unfolding data, (blue △) t = 0 points, and (blue ▽) t = ∞ points] of the refolding kinetic traces obtained from the fits. The dashed line represents the extrapolated unfolded protein signals at different GdnHCl concentrations. The solid dark red line is a fit of the equilibrium unfolding data to a two-state N ↔ U model for unfolding.[37] (c) Observed rate constants and (d) relative amplitudes for the very fast (red ○), fast (green ◇), and slow phases (light blue △) of refolding. The solid lines in panel c are fits to the data using eq 7, whereas the solid lines in panel d were drawn by inspection only. The values of the kinetic parameters describing the three phases of folding are listed in Table 1. Error bars, wherever shown, represent the spreads in the measurements taken in at least two separate experiments.

Cys42 Destabilizes the Protein at Higher pH Values. Cys42 is present in the second β-strand and seems to be completely buried with no solvent-accessible surface area. The E24A/C42A double mutant retains its native structure at pH 12,

dx.doi.org/10.1021/bi3008017 | Biochemistry 2012, 51, 9058−9066

and its stability is independent of pH in the range of 4−10. The result reveals that the destabilization of wt scMN above pH 8 is driven by the shift in the pK_a value of Cys42. The observation that for E24A, the stability decreases only above pH 8 indicates that the pK_a of Cys42 in the unfolded form of this mutant protein, and therefore most likely also in the unfolded form of wt scMN, is ∼8, which is the value expected for a cysteine thiol in water. It appears that the pK_a value of Cys42 has shifted upward to ≥9.5 in the native state of the protein. Such a shift in the pK_a value of a buried cysteine has been observed previously for other proteins.[57−59]

Modulation of the Protein Folding Kinetics by Burial of an Ionizable Residue. This study shows that the presence of a buried ionizable residue not only affects the stability of the native protein in a pH-dependent manner but also similarly affects the stability of the TS along the folding pathway. A mutation that removes the unpartnered ionizable residue from the hydrophobic core of monellin will stabilize the native state of the protein. The same mutation will stabilize the TS of folding and/or unfolding only if the ionizable residue has become buried in the TS. If only the native state but not the TS is stabilized by the mutation, then a decrease in the unfolding rate is expected. If the residue is buried less in the TS than in the native state, then the TS will be stabilized less by the mutation than would be the native state. The stabilization of the TS upon mutation can be measured by comparing the folding and unfolding rates of the mutant protein to those of its wild-type counterpart.

The folding and unfolding mechanisms of E24A and wt scMN appear to be similar. The folding and unfolding of wt scMN are known to occur along multiple parallel pathways.[29,31,39] The observation that, like in the case of wt scMN, the fluorescence change accompanying the folding reaction of E24A occurs in three observable kinetic phases suggests that the folding mechanism of E24A is similar to that of wt scMN. Unlike in the case of the folding of wt scMN, a submillisecond burst phase fluorescence change occurs during the folding of E24A. In the case of wt scMN, it is known that submillisecond folding events occur during folding[29] and that they are silent to fluorescence change. It appears that in the case of E24A these submillisecond folding events are accompanied by a fluorescence change. For both E24A (data not shown) and wt scMN,[29] the three observable kinetic phases of fluorescence change are followed by a very slow kinetic phase of folding, which is silent to fluorescence change and leads to the formation of the native protein. Hence, it appears that the folding mechanism is the same for E24A and wt scMN. The observation that, like in the case of wt scMN,[29] the fluorescence change accompanying the unfolding reaction occurs in a burst phase followed by a slow kinetic phase that can be described by a single-exponential equation suggests that the unfolding mechanism for both protein variants is the same. Furthermore, the observed rate constants for the unfolding reaction for both proteins have the same dependence on GdnHCl concentration, suggesting that the same TS is being observed in both proteins.

Glu24 Is Structured in the TS of Unfolding. The unfolding of scMN can be represented by the simple scheme $N \leftrightarrow I_U \leftrightarrow U$, where I_U is an ensemble of intermediate forms that forms rapidly from N. λ_U (eq 3) is 7-fold slower for E24A than for wt scMN (Table 1), which indicates that the height of the energy barrier is 1.2 kcal mol^{-1} greater in the wt protein (Table 2). The change in the free energy of unfolding of E24A is 2.3 kcal mol^{-1} greater than that of wt scMN. Thus, the TS of unfolding in E24A has been stabilized by 1.1 kcal mol^{-1}. The observation that the TS of unfolding is destabilized to a lesser extent by the presence of the ionizable residue than is the native protein (Table 2) suggests that Glu24 in the TS is not as structured as in the native protein.

Glu24 Is Differentially Structured in the Different Transition States Defining the Three Pathways of Folding. The observation that the rate constant of the very fast (λ_f^{vf}) folding pathway is unaffected in E24A (Table 1) suggests that Glu24 is as solvated in the TS of the very fast folding pathway as it is in U. Hence, Glu24 would have the same pK_a value in this TS that it has in U. The observation that the rate constant of the fast (λ_f^{f}) folding pathway is only ∼1.5-fold faster in E24A than it is in the wild-type protein indicates that the TS on the fast folding pathway is only marginally stabilized in the mutant protein (Table 1), suggesting that Glu24 is largely solvated in the TS of the fast pathway of folding of the wild-type protein. The slow (λ_f^{s}) folding reaction is accelerated ∼7-fold (Table 1), which indicates that its TS is stabilized by 1.1 kcal mol^{-1} in the mutant protein. Hence, the TS of the slow folding reaction appears to be structured in the vicinity of Glu24. It is possible that Glu24 becomes loosely buried by nonspecific hydrophobic collapse in the transition state of the slow folding reaction.[60,61] It should be noted that the result does not mean that the transition states along the other pathways are unstructured. In fact, the transition states along the other pathways must be similarly structured, because $m_{‡-U}$ values are comparable, but they are not structured in the vicinity of Glu24.

It therefore appears that the TS on the slow folding pathway of the wild-type protein is destabilized because the Glu24 side chain remains deprotonated at pH 7, and this charged side chain becomes at least partially buried in the TS. When folding is conducted at pH 5, the rate constants for all three folding phases were found to be the same for the wild-type and mutant proteins (data not shown) and are the same as they are for E24A at pH 7. This is expected if the Glu24 side chain is in the protonated form in the TS at pH 5 and is in the deprotonated form in the TS at pH 7. While it appears that the pK_a of Glu24 in the TS is higher than it is in U (pK_a^U = 4.5),[32] it is, unfortunately, not possible to determine with any reliable accuracy any shift in the pK_a value in the TS.

On all three folding pathways, very fast, fast, and slow, complete burial of the Glu24 side chain occurs after the transition states on the pathways. For the very fast pathway, burial begins only after the protein undergoes the transition through the TS; for the fast pathway, burial has barely started in the TS, and for the slow pathway, burial has begun before the TS is reached. On all three pathways, the observable folding phases lead to intermediates with nativelike structure (fluorescence), which fold very slowly to N.[29] This last very slow step in folding is dominated by *trans*−*cis* proline isomerization.[29] It is likely that complete burial of protonated Glu24 occurs only in the very slow phase of folding. Only those protein molecules with a protonated Glu24 will fold in the last step of folding.

Equivalence of Folding and Unfolding Pathways. While three pathways for folding have been identified for scMN at low GdnHCl concentrations, only two pathways for unfolding have been identified at high GdnHCl concentrations.[29] Under any folding condition, unfolding must occur by the same pathways by which folding occurs, and the three pathways that operate for folding must operate for unfolding as well. Each unfolding pathway would be the reverse of the corresponding folding pathway, in the sequence of structural events that occur. The observation that unfolding can be described by a simple one-

dx.doi.org/10.1021/bi3008017 | *Biochemistry* 2012, 51, 9058−9066

pathway N ↔ I_U ↔ U mechanism at high denaturant concentrations suggests that all three folding pathways are not operative at high denaturant concentrations. Indeed, for wt scMN, the amplitude of the slow folding reaction increases at the expense of the fast folding reaction with an increase in GdnHCl concentration,[29] so that the slow folding reaction is dominant at high GdnHCl concentrations.

It is possible that at low GdnHCl concentrations the flux of unfolding occurs predominantly along only one of the three folding−unfolding pathways, and hence, only one unfolding pathway is detectable. If that is the case, it would be useful to identify the observable unfolding pathway with either the very fast, fast, or slow folding pathway. It appears that the unfolding pathway observed corresponds to the reverse of the slow folding pathway. Of the three folding pathways, only the slow folding pathway, and not the very fast and fast folding pathways, resembles the unfolding pathway in being significantly affected by the Glu24 → Ala mutation (Table 1). The stabilization of the TS for the slow phase of the refolding kinetics and for the unfolding kinetics is found to be the same. The observation (Table 2 and Figure 7) that the effect of the mutation on the free energies of activation of the slow folding reaction and of the unfolding reaction predicts very well the effect of the mutation on the stability of the protein ($\Delta\Delta G^{o}_{U}$ = 2.3 kcal mol^{-1}) suggests that the slow folding reaction and the observed unfolding reaction are the reverse of each other. The coincidence of the values for $\Delta\Delta G^{o}_{U}$ obtained from kinetic and equilibrium measurements also validates the inherent assumption made in the analysis that the mutation does not perturb the free energy of the unfolded state of the protein. The kinetic m values from the folding ($m_{\ddagger-U}^{s}$) and unfolding ($m_{\ddagger-N}$) studies do not add up to the equilibrium m value (m_U). The observed difference may arise from the underestimation of the equilibrium m_U value caused by the presence of an undetected equilibrium intermediate.[62] The kinetic m value will also not equal the equilibrium m value in the case of the involvement of a proline isomerization reaction.[63]

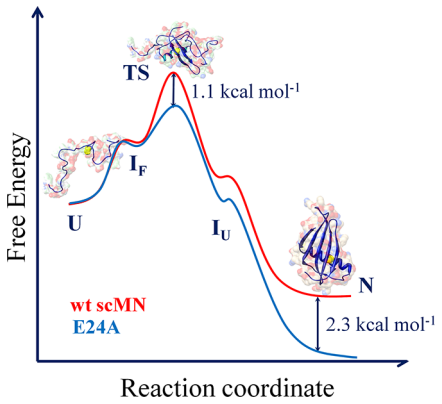

Figure 7. Effect of the Glu24 → Ala mutation on the free energy profile of the slow folding−unfolding pathway.

Characterization of the TS. The TS is a transiently populated species along the reaction path, and hence, it cannot be characterized using the conventional tools available to characterize the native state of the protein. Previously, attempts were made to characterize the TS by taking advantage of a buried ionizable residue in the core of the protein.[64−67] These studies used a pH dependence study of the wild-type protein to evaluate the structural properties of the TS, but a change in pH affects the behavior of not only the buried ionizable residue but also the overall charge distribution in the protein; thus, observations made from such studies may provide misleading information and need to be examined by more reliable approaches. Very limited studies have been conducted to characterize the TS using the approach of linkage analysis combined with ϕ-value analysis.[63] The presence of an unpartnered ionizable residue in the hydrophobic core of the structure may destabilize the structure in a pH-dependent manner. Different mutant proteins that have a buried ionizable residue located in different regions[56] of the protein can be generated to probe how different parts of the protein acquire the structure. The approach may prove to be better than previously suggested approaches[28,68,69] because of the larger change in the stability of the protein upon such mutation.[18−20,56]

Residue-specific characterization of structure in the TS is usually achieved by ϕ-value analysis[28] in which the effect of a single-residue mutation on TS stability relative to native state stability is correlated to the formation of structure by the residue in the TS relative to that in native state. Partial ϕ-values, which are commonly observed, could be due to the existence of multiple pathways, with the mutation having an effect on only one or a few of the many pathways that are operational,[70] but this explanation is usually discounted. In this study of the folding of scMN, for which multiple folding pathways had been identified previously,[29,39] it is shown that removal of an ionizable residue significantly affects the stability of the TS on only one of the three available pathways. This effect is seen because the structures of the TS on the three pathways are different in the vicinity of Glu24.

AUTHOR INFORMATION

Corresponding Author

*Phone: 91-80-23666150. Fax: 91-80-23636662. E-mail: jayant@ncbs.res.in.

Funding

This work was funded by the Tata Institute of Fundamental Research and by the Department of Science and Technology, Government of India. J.B.U. is a recipient of a J. C. Bose National Fellowship from the Government of India.

Notes

The authors declare no competing financial interest.

ACKNOWLEDGMENTS

We thank members of our laboratory for discussions. I.D. is an undergraduate student at the Indian Institute of Technology (Mumbai, India).

ABBREVIATIONS

CD, circular dichroism; dcMN, double-chain monellin; scMN, single-chain monellin; GdnHCl, guanidine hydrochloride; TS, transition state.

REFERENCES

(1) Bolen, D. W., and Rose, G. D. (2008) Structure and energetics of the hydrogen-bonded backbone in protein folding. *Annu. Rev. Biochem. 77*, 339−362.

(2) Dill, K. A. (1990) Dominant forces in protein folding. *Biochemistry 29*, 7133−7155.

(3) Kauzmann, W. (1959) Some factors in the interpretation of protein denaturation. *Adv. Protein Chem. 14*, 1−63.

(4) Tanford, C. (1962) Contribution of Hydrophobic Interactions to the Stability of the Globular Conformation of Proteins. *J. Am. Chem. Soc. 84*, 4240−4247.

(5) Privalov, P. L. (1979) Stability of proteins: Small globular proteins. *Adv. Protein Chem. 33*, 167−241.
(6) Shoemaker, K. R., Kim, P. S., York, E. J., Stewart, J. M., and Baldwin, R. L. (1987) Tests of the helix dipole model for stabilization of α-helices. *Nature 326*, 563−567.
(7) Pace, C. N. (2001) Polar group burial contributes more to protein stability than nonpolar group burial. *Biochemistry 40*, 310−313.
(8) Kumar, S., and Nussinov, R. (2002) Close-range electrostatic interactions in proteins. *ChemBioChem 3*, 604−617.
(9) Finkelstein, A. V., and Ptitsyn, O. B. (2002) *Protein Physics: A Course of Lectures*, Academic Press, Amsterdam.
(10) Yang, A.-S., and Honig, B. (1992) Electrostatic effects on protein stability. *Curr. Opin. Struct. Biol. 2*, 40−45.
(11) Matthews, B. W. (1995) Can proteins be turned inside-out? *Nat. Struct. Biol. 2*, 85−86.
(12) Schueler, O., and Margalit, H. (1995) Conservation of salt bridges in protein families. *J. Mol. Biol. 248*, 125−135.
(13) Perl, D., Mueller, U., Heinemann, U., and Schmid, F. X. (2000) Two exposed amino acid residues confer thermostability on a cold shock protein. *Nat. Struct. Biol. 7*, 380−383.
(14) Bosshard, H. R., Marti, D. N., and Jelesarov, I. (2004) Protein stabilization by salt bridges: Concepts, experimental approaches and clarification of some misunderstandings. *J. Mol. Recognit. 17*, 1−16.
(15) Kay, M. S., and Baldwin, R. L. (1998) Alternative models for describing the acid unfolding of the apomyoglobin folding intermediate. *Biochemistry 37*, 7859−7868.
(16) Fitch, C. A., Whitten, S. T., Hilser, V. J., and Garcia-Moreno, E. B. (2006) Molecular mechanisms of pH-driven conformational transitions of proteins: Insights from continuum electrostatics calculations of acid unfolding. *Proteins 63*, 113−126.
(17) Tanford, C. (1970) Protein denaturation. C. Theoretical models for the mechanism of denaturation. *Adv. Protein Chem. 24*, 1−95.
(18) Langsetmo, K., Fuchs, J. A., and Woodward, C. (1991) The conserved, buried aspartic acid in oxidized *Escherichia coli* thioredoxin has a pKa of 7.5. Its titration produces a related shift in global stability. *Biochemistry 30*, 7603−7609.
(19) Dwyer, J. J., Gittis, A. G., Karp, D. A., Lattman, E. E., Spencer, D. S., Stites, W. E., and Garcia-Moreno, E. B. (2000) High apparent dielectric constants in the interior of a protein reflect water penetration. *Biophys. J. 79*, 1610−1620.
(20) Isom, D. G., Castaneda, C. A., Cannon, B. R., Velu, P. D., and Garcia-Moreno, E. B. (2010) Charges in the hydrophobic interior of proteins. *Proc. Natl. Acad. Sci. U.S.A. 107*, 16096−16100.
(21) Garcia-Seisdedos, H., Ibarra-Molero, B., and Sanchez-Ruiz, J. M. (2012) How many ionizable groups can sit on a protein hydrophobic core? *Proteins 80*, 1−7.
(22) Karp, D. A., Gittis, A. G., Stahley, M. R., Fitch, C. A., Stites, W. E., and Garcia-Moreno, E. B. (2007) High apparent dielectric constant inside a protein reflects structural reorganization coupled to the ionization of an internal Asp. *Biophys. J. 92*, 2041−2053.
(23) Harms, M. J., Castaneda, C. A., Schlessman, J. L., Sue, G. R., Isom, D. G., Cannon, B. R., and Garcia-Moreno, E. B. (2009) The pK_a values of acidic and basic residues buried at the same internal location in a protein are governed by different factors. *J. Mol. Biol. 389*, 34−47.
(24) Varadarajan, R., Lambright, D. G., and Boxer, S. G. (1989) Electrostatic interactions in wild-type and mutant recombinant human myoglobins. *Biochemistry 28*, 3771−3781.
(25) Stites, W. E., Gittis, A. G., Lattman, E. E., and Shortle, D. (1991) In a staphylococcal nuclease mutant the side-chain of a lysine replacing valine 66 is fully buried in the hydrophobic core. *J. Mol. Biol. 221*, 7−14.
(26) Garcia-Moreno, B., Dwyer, J. J., Gittis, A. G., Lattman, E. E., Spencer, D. S., and Stites, W. E. (1997) Experimental measurement of the effective dielectric in the hydrophobic core of a protein. *Biophys. Chem. 64*, 211−224.
(27) Fitch, C. A., Karp, D. A., Lee, K. K., Stites, W. E., Lattman, E. E., and Garcia-Moreno, E. B. (2002) Experimental pK_a values of buried residues: Analysis with continuum methods and role of water penetration. *Biophys. J. 82*, 3289−3304.
(28) Matouschek, A., Kellis, J. T., Jr., Serrano, L., and Fersht, A. R. (1989) Mapping the transition state and pathway of protein folding by protein engineering. *Nature 340*, 122−126.
(29) Patra, A. K., and Udgaonkar, J. B. (2007) Characterization of the folding and unfolding reactions of single-chain monellin: Evidence for multiple intermediates and competing pathways. *Biochemistry 46*, 11727−11743.
(30) Jha, S. K., and Udgaonkar, J. B. (2009) Direct evidence for a dry molten globule intermediate during the unfolding of a small protein. *Proc. Natl. Acad. Sci. U.S.A. 106*, 12289−12294.
(31) Jha, S. K., Dhar, D., Krishnamoorthy, G., and Udgaonkar, J. B. (2009) Continuous dissolution of structure during the unfolding of a small protein. *Proc. Natl. Acad. Sci. U.S.A. 106*, 11113−11118.
(32) Aghera, N., Earanna, N., and Udgaonkar, J. B. (2011) Equilibrium unfolding studies of monellin: The double-chain variant appears to be more stable than the single-chain variant. *Biochemistry 50*, 2434−2444.
(33) Xue, W. F., Carey, J., and Linse, S. (2004) Multi-method global analysis of thermodynamics and kinetics in reconstitution of monellin. *Proteins 57*, 586−595.
(34) Xue, W. F., Szczepankiewicz, O., Bauer, M. C., Thulin, E., and Linse, S. (2006) Intra- versus intermolecular interactions in monellin: Contribution of surface charges to protein assembly. *J. Mol. Biol. 358*, 1244−1255.
(35) Aghera, N., and Udgaonkar, J. B. (2012) Kinetic Studies of the Folding of Heterodimeric Monellin: Evidence for Switching between Alternative Parallel Pathways. *J. Mol. Biol. 420*, 235−250.
(36) Aghera, N., and Udgaonkar, J. B. (2011) Heterologous expression, purification and characterization of heterodimeric monellin. *Protein Expression Purif. 76*, 248−253.
(37) Agashe, V. R., and Udgaonkar, J. B. (1995) Thermodynamics of denaturation of barstar: Evidence for cold denaturation and evaluation of the interaction with guanidine hydrochloride. *Biochemistry 34*, 3286−3299.
(38) Kimura, T., Maeda, A., Nishiguchi, S., Ishimori, K., Morishima, I., Konno, T., Goto, Y., and Takahashi, S. (2008) Dehydration of main-chain amides in the final folding step of single-chain monellin revealed by time-resolved infrared spectroscopy. *Proc. Natl. Acad. Sci. U.S.A. 105*, 13391−13396.
(39) Jha, S. K., Dasgupta, A., Malhotra, P., and Udgaonkar, J. B. (2011) Identification of multiple folding pathways of monellin using pulsed thiol labeling and mass spectrometry. *Biochemistry 50*, 3062−3074.
(40) Nozaki, Y., and Tanford, C. (1963) The Solubility of Amino Acids and Related Compounds in Aqueous Urea Solutions. *J. Biol. Chem. 238*, 4074−4081.
(41) Nozaki, Y., and Tanford, C. (1971) The solubility of amino acids and two glycine peptides in aqueous ethanol and dioxane solutions. Establishment of a hydrophobicity scale. *J. Biol. Chem. 246*, 2211−2217.
(42) Cornette, J. L., Cease, K. B., Margalit, H., Spouge, J. L., Berzofsky, J. A., and DeLisi, C. (1987) Hydrophobicity scales and computational techniques for detecting amphipathic structures in proteins. *J. Mol. Biol. 195*, 659−685.
(43) Wimley, W. C., Creamer, T. P., and White, S. H. (1996) Solvation energies of amino acid side chains and backbone in a family of host-guest pentapeptides. *Biochemistry 35*, 5109−5124.
(44) Perutz, M. F., Kendrew, J. C., and Watson, H. C. (1965) Structure and function of haemoglobin: II. Some relations between polypeptide chain configuration and amino acid sequence. *J. Mol. Biol. 13*, 669−678.
(45) Lee, B., and Richards, F. M. (1971) The interpretation of protein structures: Estimation of static accessibility. *J. Mol. Biol. 55*, 379−400.
(46) Warshel, A. (1978) Energetics of enzyme catalysis. *Proc. Natl. Acad. Sci. U.S.A. 75*, 5250−5254.
(47) Abrahams, J. P., Leslie, A. G., Lutter, R., and Walker, J. E. (1994) Structure at 2.8 Å resolution of F1-ATPase from bovine heart mitochondria. *Nature 370*, 621−628.
(48) Bogan, A. A., and Thorn, K. S. (1998) Anatomy of hot spots in protein interfaces. *J. Mol. Biol. 280*, 1−9.
(49) Bartlett, G. J., Porter, C. T., Borkakoti, N., and Thornton, J. M. (2002) Analysis of catalytic residues in enzyme active sites. *J. Mol. Biol. 324*, 105−121.

(50) Jiang, Y., Ruta, V., Chen, J., Lee, A., and MacKinnon, R. (2003) The principle of gating charge movement in a voltage-dependent K^+ channel. *Nature 423*, 42−48.
(51) Bush, J., and Makhatadze, G. I. (2011) Statistical analysis of protein structures suggests that buried ionizable residues in proteins are hydrogen bonded or form salt bridges. *Proteins 79*, 2027−2032.
(52) Rashin, A. A., and Honig, B. (1984) On the environment of ionizable groups in globular proteins. *J. Mol. Biol. 173*, 515−521.
(53) Chakravarty, S., and Varadarajan, R. (1999) Residue depth: A novel parameter for the analysis of protein structure and stability. *Structure 7*, 723−732.
(54) Giletto, A., and Pace, C. N. (1999) Buried, charged, non-ion-paired aspartic acid 76 contributes favorably to the conformational stability of ribonuclease T1. *Biochemistry 38*, 13379−13384.
(55) Grimsley, G. R., Scholtz, J. M., and Pace, C. N. (2009) A summary of the measured pK values of the ionizable groups in folded proteins. *Protein Sci. 18*, 247−251.
(56) Isom, D. G., Castaneda, C. A., Cannon, B. R., and Garcia-Moreno, B. (2011) Large shifts in pK_a values of lysine residues buried inside a protein. *Proc. Natl. Acad. Sci. U.S.A. 108*, 5260−5265.
(57) Khurana, R., Hate, A. T., Nath, U., and Udgaonkar, J. B. (1995) pH dependence of the stability of barstar to chemical and thermal denaturation. *Protein Sci. 4*, 1133−1144.
(58) Pinitglang, S., Watts, A. B., Patel, M., Reid, J. D., Noble, M. A., Gul, S., Bokth, A., Naeem, A., Patel, H., Thomas, E. W., Sreedharan, S. K., Verma, C., and Brocklehurst, K. (1997) A classical enzyme active center motif lacks catalytic competence until modulated electrostatically. *Biochemistry 36*, 9968−9982.
(59) Tolbert, B. S., Tajc, S. G., Webb, H., Snyder, J., Nielsen, J. E., Miller, B. L., and Basavappa, R. (2005) The active site cysteine of ubiquitin-conjugating enzymes has a significantly elevated pK_a: Functional implications. *Biochemistry 44*, 16385−16391.
(60) Anil, B., Sato, S., Cho, J. H., and Raleigh, D. P. (2005) Fine structure analysis of a protein folding transition state; distinguishing between hydrophobic stabilization and specific packing. *J. Mol. Biol. 354*, 693−705.
(61) Farber, P. J., and Mittermaier, A. (2008) Side chain burial and hydrophobic core packing in protein folding transition states. *Protein Sci. 17*, 644−651.
(62) Spudich, G., and Marqusee, S. (2000) A change in the apparent m value reveals a populated intermediate under equilibrium conditions in *Escherichia coli* ribonuclease HI. *Biochemistry 39*, 11677−11683.
(63) Horng, J. C., Cho, J. H., and Raleigh, D. P. (2005) Analysis of the pH-dependent folding and stability of histidine point mutants allows characterization of the denatured state and transition state for protein folding. *J. Mol. Biol. 345*, 163−173.
(64) Oliveberg, M., and Fersht, A. R. (1996) New approach to the study of transient protein conformations: The formation of a semiburied salt link in the folding pathway of barnase. *Biochemistry 35*, 6795−6805.
(65) Luisi, D. L., and Raleigh, D. P. (2000) pH-dependent interactions and the stability and folding kinetics of the N-terminal domain of L9. Electrostatic interactions are only weakly formed in the transition state for folding. *J. Mol. Biol. 299*, 1091−1100.
(66) Jamin, M., Geierstanger, B., and Baldwin, R. L. (2001) The pK_a of His-24 in the folding transition state of apomyoglobin. *Proc. Natl. Acad. Sci. U.S.A. 98*, 6127−6131.
(67) Sato, S., and Raleigh, D. P. (2002) pH-dependent stability and folding kinetics of a protein with an unusual $\alpha\beta$ topology: The C-terminal domain of the ribosomal protein L9. *J. Mol. Biol. 318*, 571−582.
(68) Krantz, B. A., Dothager, R. S., and Sosnick, T. R. (2004) Discerning the structure and energy of multiple transition states in protein folding using ψ-analysis. *J. Mol. Biol. 337*, 463−475.
(69) Mitra, L., Hata, K., Kono, R., Maeno, A., Isom, D., Rouget, J. B., Winter, R., Akasaka, K., Garcia-Moreno, B., and Royer, C. A. (2007) V(i)-value analysis: A pressure-based method for mapping the folding transition state ensemble of proteins. *J. Am. Chem. Soc. 129*, 14108−14109.
(70) Zaidi, F. N., Nath, U., and Udgaonkar, J. B. (1997) Multiple intermediates and transition states during protein unfolding. *Nat. Struct. Biol. 4*, 1016−1024.